Hindawi Publishing Corporation
Journal of Nanomaterials
Volume 2016, Article ID 1827151, 7 pages
http://dx.doi.org/10.1155/2016/1827151

*Research Article*

# Efficient Photoelectrochemical Water Oxidation by Metal-Doped Bismuth Vanadate Photoanode with Iron Oxyhydroxide Electrocatalyst

**Eun Jin Joo, Gisang Park, Ji Seon Gwak, Jong Hyeok Seo, Kyu Yeon Jang, Kyung Hee Oh, and Ki Min Nam**

*Department of Chemistry, Mokpo National University, Jeonnam 534-729, Republic of Korea*

Correspondence should be addressed to Ki Min Nam; namkimin.chem@gmail.com

Received 18 February 2016; Accepted 27 April 2016

Academic Editor: Vincenzo Baglio



Intensive attention has been currently focused on the discovery of semiconductor and proficient cocatalysts for eventual applications to the photoelectrochemical water splitting system. A W-Mo-doped $BiVO_4$ semiconductor was prepared by the surfactant-assisted thermal decomposition method on a fluorine-doped tin oxide conductive film. The W-Mo-doped $BiVO_4$ films showed a porous morphology with the grain sizes of about 270 nm. Because the hole diffusion length of $BiVO_4$ is about 100 nm, the W-Mo-doped $BiVO_4$ film in this study is an ideal candidate for the photoelectrochemical water oxidation. Iron oxyhydroxide (FeOOH) electrocatalyst was chemically deposited on the W-Mo-doped $BiVO_4$ to investigate the effect of the electrocatalyst on the semiconductor. The W-Mo-doped $BiVO_4$/FeOOH composite electrode showed enhanced activity compared to the pristine W-Mo-doped $BiVO_4$ electrode for water oxidation reaction. The chemical deposition is a promising method for the deposition of FeOOH on semiconductor.

## 1. Introduction

Photoelectrochemical (PEC) water splitting using semiconductor electrode is a promising method of converting solar energy to chemical fuel [1, 2]. Among the various semiconductor materials, metal oxides such as $TiO_2$, $WO_3$, $Fe_2O_3$, and $BiVO_4$ have gained significant interest owing to their photochemical stability and low cost. However, they have a low PEC efficiency compared to the theoretical values, because of significant electron-hole recombination and slow surface kinetics [3, 4]. While a multitude of methods such as doping, morphology control, making composite structure, and adding electrocatalysts have been investigated for the improvement in PEC water splitting [5–8], achievement of theoretical conversion efficiency is still far from being reached.

$BiVO_4$ has been intensively studied as a photoanode (n-type semiconductor) for PEC water oxidation, because it absorbs a large portion of the visible light and has a favorable valence band edge [9–11]. However, the slow carrier mobility in the bulk as well as fast recombination at the surface contributes to the poor water oxidation efficiency of $BiVO_4$. The introduction of dopant such as W and Mo into $BiVO_4$ has been found to enhance the PEC performance [12, 13]. The dopant in $BiVO_4$ can increase n-type conductivity and could significantly enhance the PEC activity. Furthermore, W and Mo codoping (W-Mo-doped $BiVO_4$) has shown better performance than W or Mo alone for the $BiVO_4$ [14]. Nanostructure can also enhance the kinetic parameters of the water oxidation reactions through the discrimination of bulk recombinations. For efficient PEC water oxidation, $BiVO_4$ requires both particles smaller than its hole diffusion length (~100 nm) [11] and the introduction of proper dopants. However, those are still not sufficient to overcome the low surface kinetic of $BiVO_4$.

Recently, proficient electrocatalysts for eventual PEC applications have been intensively studied, but there is no guarantee that the best electrocatalysts will perform equally

when integrated into a PEC water splitting system [15, 16]. The source of catalytic improvement of electrocatalyst on semiconductor is not yet fully understood [17, 18]. The nature of the loaded catalysts and their interaction with the semiconductor are important to further study the PEC water splitting. Recently, a number of studies have focused on the potential applications of iron oxyhydroxide (FeOOH) as the cocatalysts [15]. Unfortunately, most of the researches considered to date have only focused on the photodeposition or electrodeposition method [7, 15].

In this study, we report a facile formation of W-Mo-doped $BiVO_4$ films on fluorine-doped tin oxide (FTO) for the PEC water oxidation. The W-Mo-doped $BiVO_4$ films showed a porous morphology with the grain sizes of about 270 nm. Because the hole diffusion length of $BiVO_4$ is about 100 nm, the W-Mo-doped $BiVO_4$ film in this study is an ideal candidate for effective charge separation. Furthermore, FeOOH cocatalyst was chemically deposited on the W-Mo-doped $BiVO_4$ films by the oxidation of $FeSO_4$ to investigate the effect of electrocatalysts on the semiconductor surface. The W-Mo-doped $BiVO_4$/FeOOH composites showed enhanced PEC water oxidation performance.

## 2. Experimental Procedures

*2.1. Materials.* Fluorine-doped tin oxide (FTO, TEC 15, WY-GMS) coated glass was used as the substrate for the thin film electrodes. $(NH_4)_6H_2W_{12}O_{40}{\cdot}xH_2O$ (≥99.0%, Sigma-Aldrich), $Bi(NO_3)_3{\cdot}5H_2O$ (99.999%, Sigma-Aldrich), $(NH_4)_6Mo_7O_{24}{\cdot}4H_2O$ (99.98%, Sigma-Aldrich), and $VCl_3$ (99%, Alfa-Aesar) were used as the metal precursor salts and used as received. In addition, Nafion (5%, Sigma-Aldrich) and NaOCl (10%), $Na_2SO_4$, $Na_2SO_3$, $Na_2HPO_4$, $NaH_2PO_4$, ethylene glycol (99.0%), acetone (99.0%), and ethanol (99.5%) were purchased from Daejung Chemicals (Korea). Deionized (DI) water was used as the solvent in electrochemical experiments.

*2.2. Preparation of W-Mo-Doped $BiVO_4$ and Undoped $BiVO_4$ Electrodes.* FTO substrates were first cleaned in deionized water and ethanol and then sonicated in ethanol for at least 1 h. A drop-casting technique was used to create the thin film electrodes. Here, 10 mM W-Mo-doped $BiVO_4$ precursor (the atomic ratio in between Bi, V, W, and Mo was 4.6 : 4.6 : 0.2 : 0.6) in ethylene glycol solution was prepared. Nafion solution was added to the precursor solution (volume ratio between precursor and Nafion solution was 1 : 5) and then applied onto an FTO substrate. The prepared films were annealed at 500°C for 3 h (with a 3 h ramp time) in air to form the W-Mo-doped $BiVO_4$ thin film. The existence of Nafion in precursor solution tends to give reproducible growth on FTO substrate. For undoped $BiVO_4$ precursor, the atomic ratio in between Bi and V was 1 : 1 in ethylene glycol.

*2.3. Chemical Deposition of FeOOH on W-Mo-Doped $BiVO_4$ Film.* Chemical deposition of FeOOH was carried out by adding 30 mL of 1.5 M NaOCl to 15 mL of 1.0 M $FeSO_4$ solution. The solution was kept at 30°C for 3 h in air in the presence of W-Mo-doped $BiVO_4$ film, and the resulting W-Mo-doped $BiVO_4$/FeOOH electrode was washed with ethanol and DI water. FeOOH was also deposited on undoped $BiVO_4$ with the same method.

*2.4. Photodeposition of FeOOH on W-Mo-Doped $BiVO_4$ Film.* Photodeposition of FeOOH on the W-Mo-doped $BiVO_4$ was carried out in a 0.1 M $FeSO_4$ solution using a three-electrode cell setup. For the photodeposition, an external bias of 0.3 V versus Ag/AgCl was applied. The light was illuminated through the FTO side (backside) with the light intensity of 100 mW/cm$^2$. Photodeposition was performed for 30 min, and the electrode was washed with ethanol and DI water.

*2.5. Electrochemical Characterization of Electrodes.* Electrochemical characterization was performed in a specially designed cell in a three-electrode configuration with the thin film as the working electrode, a Pt wire counter electrode, and an Ag/AgCl reference electrode. The working electrode with the actual geometric area of 0.28 cm$^2$ was exposed to electrolyte solution. A 150 W xenon lamp (ABET Technologies) was used as the light source in the PEC characterization step, and light illumination area was 0.28 cm$^2$. Chopped light linear sweep voltammetry (LSV) was utilized to obtain the photocurrent responses using a DY2321 potentiostat (Digi-Ivy). The light chopping frequency was set at 2 Hz and the PEC measurements were performed by backside illumination in aqueous solutions of 0.1 M $Na_2SO_4$ with a phosphate buffer (pH 7) for water oxidation. In all tests, the intensity of the lamp on the sample was measured to be 100 mW/cm$^2$ using a Si solar cell (AIST). A 425 nm long-pass filter was used to cut the UV portion of the spectrum and to provide only visible light illumination. A monochromator (ORIEL) was used to obtain the action spectra of photoresponse as a function of wavelength. Because the preparation of W-Mo-doped $BiVO_4$ electrode is reproducible, it always shows the same photocurrents of each sample.

*2.6. Materials Characterization of Electrodes.* UV-Vis absorption spectra were acquired with a Lambda 3B Spectrophotometer (Perkin-Elmer) for wavelengths from 300 to 900 nm. The thin film electrodes were characterized by scanning electron microscopy (SEM, Philips XL30SFEG operated at 10 and 30 kV). The X-ray diffraction data was measured using Cu $K_\alpha$ radiations at 40 kV and 100 mA (Rigaku, Dmax-RB diffractometer). X-ray photoelectron spectroscopy (XPS) measurements were taken using a $K_\alpha$ spectrometer with an X-ray source of Al $K_\alpha$ and at a pass energy level of 40 eV.

## 3. Results and Discussion

*3.1. Preparation of W-Mo-Doped $BiVO_4$ Electrode.* For the facile preparation of W-Mo-doped $BiVO_4$ structure, thin film electrodes were prepared by surfactant-assisted thermal decomposition method on an FTO substrate. Figure 1(a) shows the scanning electron microscopy (SEM) of the W-Mo-doped $BiVO_4$ thin film electrode, indicating a porous

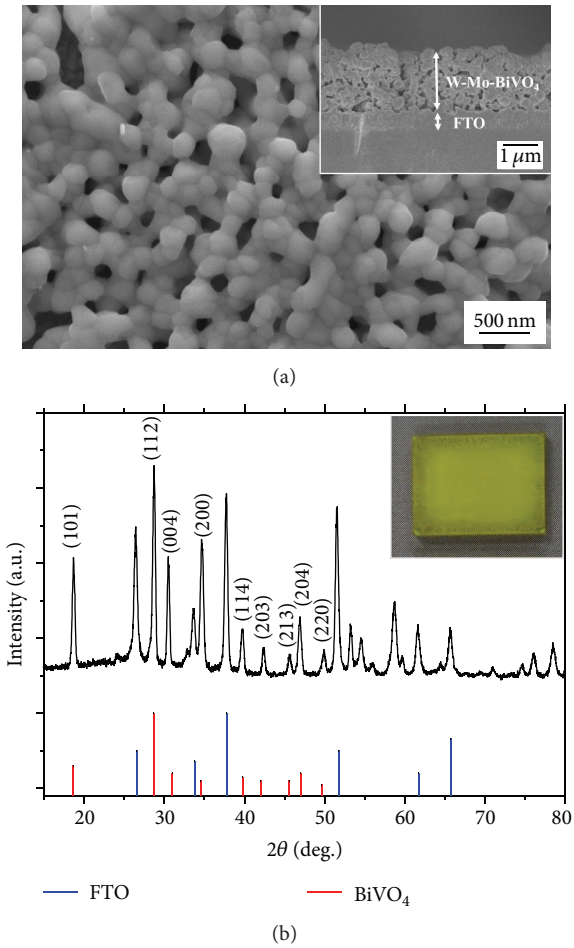


FIGURE 1: (a) SEM top-view and cross section image (inset) of the W-Mo-doped $BiVO_4$, (b) XRD patterns of the W-Mo-doped $BiVO_4$ (red line) and FTO substrate (blue line), and photographic image (inset) of the W-Mo-doped $BiVO_4$.

network with the grain sizes of 274.8 ± 63.7 nm. The cross section SEM image of the W-Mo-doped $BiVO_4$ shows the film with a thickness of about 1.1 $\mu$m (inset). The porous structures can allow the electrolyte to easily diffuse within the $BiVO_4$, increasing the contact area and shortening the hole diffusion distance [13]. Because the hole diffusion length of $BiVO_4$ is about 100 nm [11], the W-Mo-doped $BiVO_4$ thin film in this study is ideal for effective charge separation. Notably, the precursor solution without Nafion increased the grain sizes of the W-Mo-doped $BiVO_4$ and irregularly formed on the FTO substrate (351.5 ± 82.8 nm, see Figure S1 in Supplementary Material available online at http://dx.doi.org/10.1155/2016/1827151). The existence of Nafion in the precursor solution tends to provide small grain sizes as well as uniform growth on the FTO substrate (Figure 1(b) inset). The X-ray diffraction (XRD) peaks corresponded to the monoclinic structure of $BiVO_4$ (Figure 1(b)). Any secondary phase in the XRD patterns was not observed. However, a shift and merging of the XRD peaks at 34, 47, and 59° were observed, indicating that W and Mo were well dissolved in the $BiVO_4$ solid solution [14].

*3.2. PEC at the W-Mo-Doped $BiVO_4$ Electrode.* The PEC performance of the W-Mo-doped $BiVO_4$ thin film electrode was studied by linear sweep voltammetry (LSV) for both sulfite oxidation (0.1 M $Na_2SO_3$ + 0.1 M $Na_2SO_4$) and water oxidation (0.1 M $Na_2SO_4$ + 0.1 M phosphate buffered, pH 7). The LSV was conducted from −0.6 to +0.8 V versus Ag/AgCl at a scan rate of 20 mV/s with chopped light under UV-visible and visible (>425 nm) irradiations (Figure 2). The W-Mo-doped $BiVO_4$ electrode successfully generated anodic photocurrents (n-type character). Because the sulfite oxidation has extremely fast oxidation kinetics, the surface recombination is negligible [14, 15]. The sulfite oxidation is thermodynamically and kinetically favorable, and thus it has a more negative onset potential compared to that of water oxidation (Figure 2). An early onset potential (−0.5 V versus Ag/AgCl) and a rapid increase in photocurrent of 1.6 mA/cm$^2$ (0.6 V versus Ag/AgCl ) for sulfite oxidation on the W-Mo-doped $BiVO_4$ electrode indicated an excellent fill factor. However, nanosized structures are also associated with significant disadvantages, such as an increased number of grain boundaries and a reduced space-charge region [19], resulting in much lower efficiency of the W-Mo-doped $BiVO_4$ electrode than the theoretical value (7.5 mA/cm$^2$) [20]. Furthermore, the photocurrent from the W-Mo-doped $BiVO_4$ electrode for water oxidation is far lower than that of sulfite oxidation. The significant reduction in photocurrent demonstrates that the water oxidation on the W-Mo-doped $BiVO_4$ electrode is mainly limited by poor water oxidation kinetics on the electrode surface. This result indicates that a considerably improved photocurrent can be possible when the W-Mo-doped $BiVO_4$ electrode is coupled with a proper water oxidation cocatalyst.

*3.3. Chemical Deposition of FeOOH on the W-Mo-Doped $BiVO_4$ Electrode.* Efficient PEC water splitting requires both highly active semiconductor photoelectrode and proficient electrocatalyst, that is, cocatalyst. Catalyst-modified $BiVO_4$ enhanced PEC efficiency and also noticeably improved the stability [7, 21]. Recently, a number of studies have focused on the potential applications of FeOOH as the cocatalyst [15]. Unfortunately, most of the researches considered to date have only used the photodeposition or electrodeposition method on the semiconductor [7, 15].

To improve water oxidation kinetics, a thin layer of FeOOH catalyst was chemically deposited. The chemical deposition of FeOOH on the W-Mo-doped $BiVO_4$ electrode was carried out in a 1.0 M $FeSO_4$ with 1.5 M NaOCl solution. $FeSO_4$ was oxidized to FeOOH by the NaOCl reduction reaction [22] and then deposited on the W-Mo-doped $BiVO_4$ electrode. $Fe^{3+}$ ions are insoluble in an aqueous medium [23] and thus precipitated as FeOOH on the W-Mo-doped $BiVO_4$ electrode. As-deposited FeOOH film was amorphous. To determine the chemical state of the film, X-ray photoelectron spectroscopy (XPS) was performed (Figure 3). In the Fe $2p_{1/2}$ and Fe $2p_{3/2}$ region, the spectra have three major peaks assigned at 724, 718, and 712.5 eV for $Fe^{3+}$ [24, 25]. In the O 1s region, the lowest binding energy peak at 529.7 eV can be

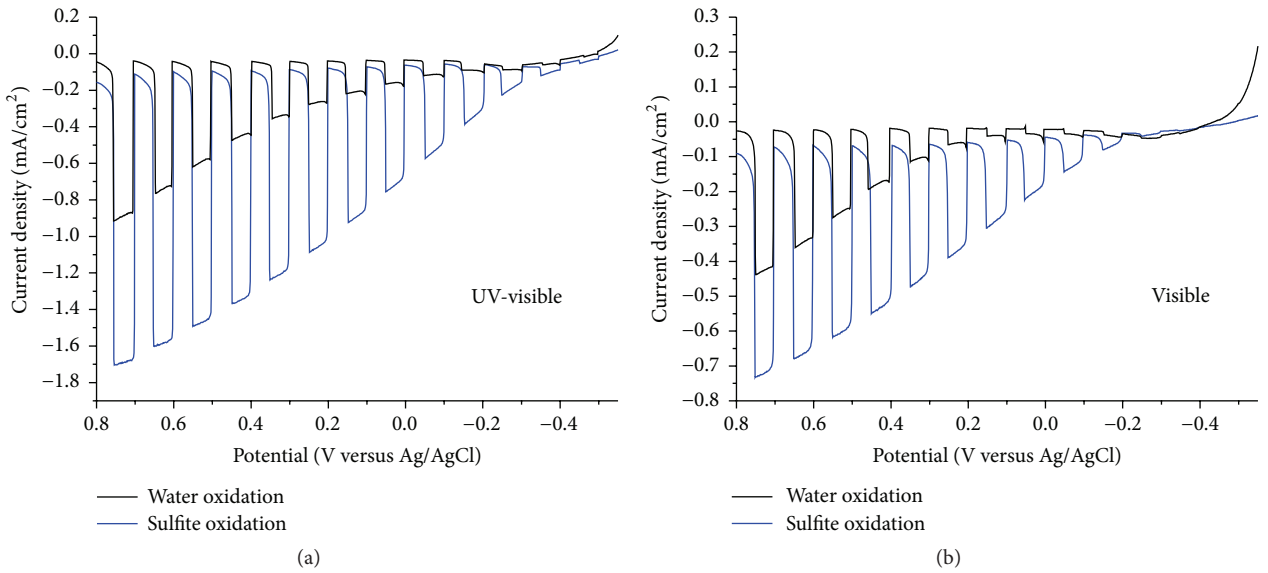


FIGURE 2: LSVs for the sulfite oxidation (0.1 M $Na_2SO_3$ + 0.1 M $Na_2SO_4$) and water oxidation (0.1 M $Na_2SO_4$ + 0.1 M phosphate buffered, pH 7) using the W-Mo-doped $BiVO_4$ under (a) UV-visible and (b) visible light irradiation. Scan rate: 20 mV/s. Light intensity: 100 mW/cm$^2$.

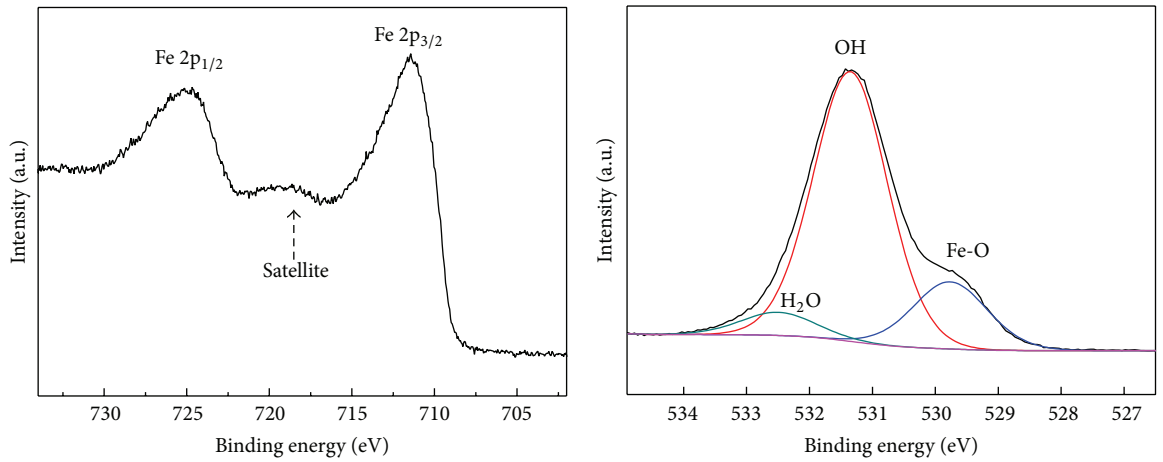


FIGURE 3: XPS spectra of the FeOOH on the W-Mo-doped $BiVO_4$ in the (a) Fe 2p and (b) O 1s regions.

assigned to oxygen atoms in the iron oxide lattice, O 1s (Fe-O), and the peak at 532.1 eV is assigned to lattice hydroxyl group, O 1s (Fe-OH), that matched well with FeOOH spectra [24]. Figure 4 shows the SEM image of FeOOH on the W-Mo-doped $BiVO_4$ (W-Mo-doped $BiVO_4$/FeOOH), indicating that FeOOH was uniformly covered on the electrode surface, while maintaining the shape of the W-Mo-doped $BiVO_4$. This method is simple and cost effective compared to electrodeposition or photodeposition.

*3.4. PEC at the W-Mo-Doped $BiVO_4$/FeOOH Electrode.* The photocurrents for water oxidation from the resulting W-Mo-doped $BiVO_4$/FeOOH electrode were significantly higher than that of the W-Mo-doped $BiVO_4$ electrode (Figure 5). The W-Mo-doped $BiVO_4$/FeOOH composite electrode attained almost 2-fold higher photocurrent than the W-Mo-doped $BiVO_4$ for water oxidation reaction at +0.6 V versus Ag/AgCl. The onset potential of W-Mo-doped $BiVO_4$/FeOOH electrode is slightly shifted to the negative direction indicating reduced surface recombination processes at the small overpotential value. The action spectra of the W-Mo-doped $BiVO_4$/FeOOH electrode show typical photocurrents at +0.3 V versus Ag/AgCl depending on the wavelength with a 10 nm interval (Figure 6). The bandgaps were determined from the wavelengths for the onset of photocurrent. The W-Mo-doped $BiVO_4$/FeOOH showed the same onset wavelength as that of the W-Mo-doped $BiVO_4$ (540 nm), indicating that the bandgap of W-Mo-doped $BiVO_4$/FeOOH did not

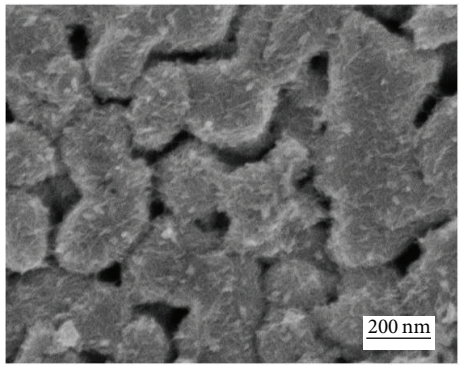


Figure 4: SEM image of FeOOH on the W-Mo-doped $BiVO_4$.

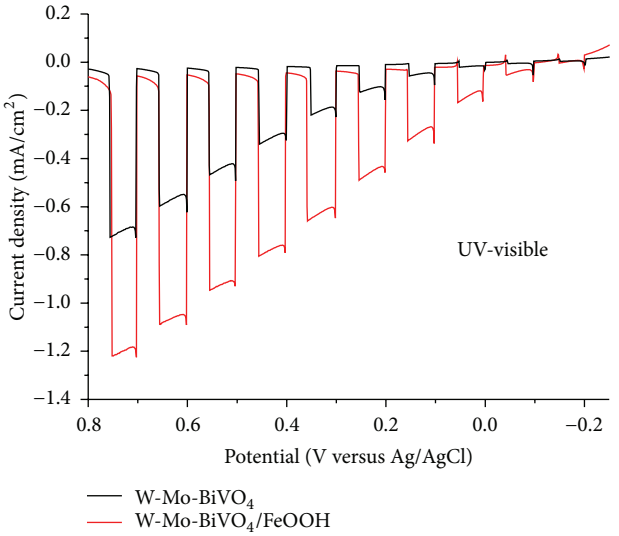


Figure 5: LSVs of the W-Mo-doped $BiVO_4$ and W-Mo-doped $BiVO_4$/FeOOH electrodes under UV-visible illumination in phosphate buffer (pH 7). Scan rate: 20 mV/s. Light intensity: 100 mW/cm$^2$.

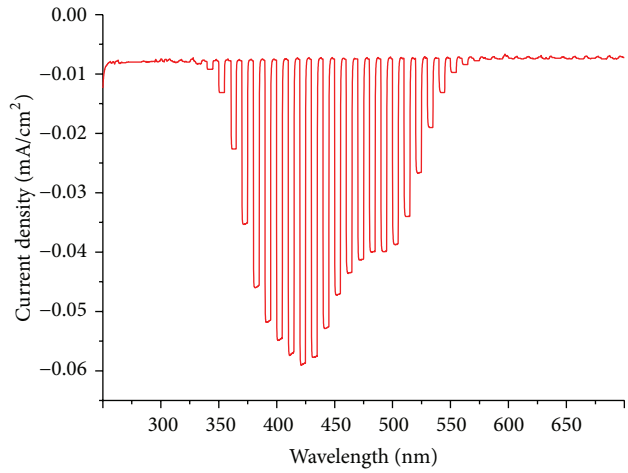


Figure 6: Action spectrum of the W-Mo-doped $BiVO_4$/FeOOH electrode at an applied potential of 0.3 V versus Ag/AgCl under UV-visible illumination in phosphate buffer (pH 7).

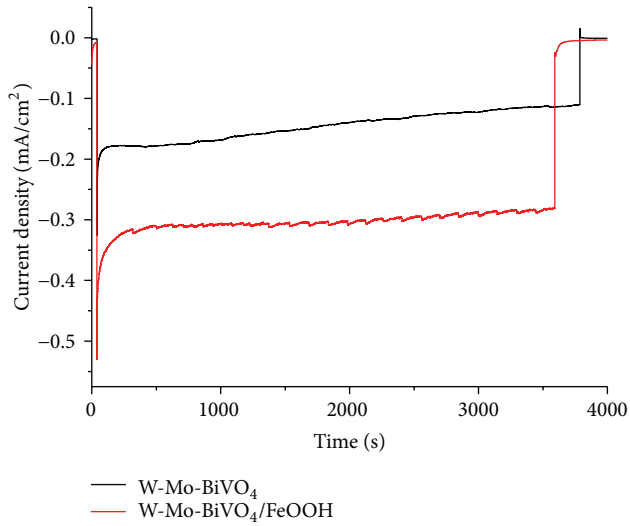


Figure 7: Current-time response curves of the W-Mo-doped $BiVO_4$, and W-Mo-doped $BiVO_4$/FeOOH electrodes at an applied potential of 0.3 V versus Ag/AgCl in phosphate buffer (pH 7).

change (Figure S2(a)). The bandgap can also be estimated from the onset of the UV-visible absorbance spectrum (Figure S2(b)). From the absorbance data, the W-Mo-doped $BiVO_4$ sample showed direct transitions with the bandgaps of ~2.4 eV. The bandgap obtained from the absorbance agrees well with the action spectrum data, and the onset wavelength of the W-Mo-doped $BiVO_4$ is essentially the same.

To assess the stability of both the W-Mo-doped $BiVO_4$ and W-Mo-doped $BiVO_4$/FeOOH electrodes over time, chronoamperometry was carried out at +0.3 V versus Ag/AgCl under UV-visible irradiation (Figure 7). After an initial drop, the photocurrent of the W-Mo-doped $BiVO_4$/FeOOH was stabilized at a steady-state value of 0.3 mA/cm$^2$ at 0.3 V versus Ag/AgCl. The presence of FeOOH electrocatalyst effectively suppresses the photochemical deactivation of the W-Mo-doped $BiVO_4$. This result demonstrates the promise of chemically deposited FeOOH electrocatalyst for improving the photocurrent as well as the stability of the W-Mo-doped $BiVO_4$. Furthermore, when FeOOH catalyst was deposited on undoped $BiVO_4$, the photocurrent also showed significantly enhanced PEC efficiency (Figure 8).

For comparison, a FeOOH layer was photodeposited on the W-Mo-doped $BiVO_4$ electrode. The photocurrents for water oxidation from the resulting W-Mo-doped $BiVO_4$/FeOOH electrode also showed enhanced activity compared to that of the W-Mo-doped $BiVO_4$ electrode (Figure S3). The photocurrent of chemically deposited FeOOH on the W-Mo-doped $BiVO_4$ showed a slightly higher value than that of photodeposited FeOOH sample, indicating that the chemical deposition can be an alternative method for the preparation of semiconductor-FeOOH composite for PEC water oxidation. This result indicates that the chemically deposited FeOOH is promising for improving the PEC activity for water oxidation.

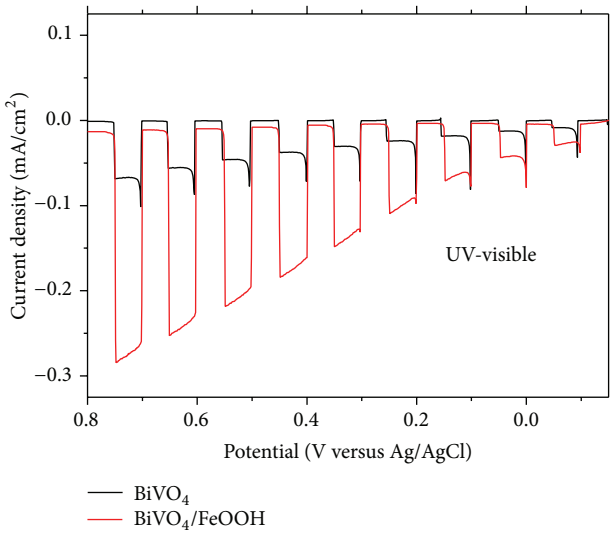


FIGURE 8: LSVs of $BiVO_4$ and $BiVO_4$/FeOOH electrodes under UV-visible illumination in phosphate buffer (pH 7). Scan rate: 20 mV/s. Light intensity: 100 mW/cm$^2$.

## 4. Conclusions

A W-Mo-doped $BiVO_4$ semiconductor was prepared by Nafion-assisted thermal decomposition method on an FTO substrate. The W-Mo-doped $BiVO_4$ electrodes showed a porous network with the grain sizes of ~270 nm. Because the hole diffusion length of $BiVO_4$ is about 100 nm, the $BiVO_4$ film in this study was found to be ideal for effective charge separation. FeOOH electrocatalyst was chemically deposited by the oxidation of $FeSO_4$ on the W-Mo-doped $BiVO_4$. The W-Mo-doped $BiVO_4$/FeOOH composite electrode attained at least 2-fold higher photocurrent at 0.3 V (versus Ag/AgCl) than that of the W-Mo-doped $BiVO_4$ for water oxidation reaction. Furthermore, the W-Mo-doped $BiVO_4$/FeOOH composite showed high photochemical stability. This result demonstrates that the chemically deposited FeOOH is promising for improving the activity as well as the stability of the water oxidation reaction.

## Competing Interests

The authors declare that there is no conflict of interests regarding the publication of this paper.

## Acknowledgments

This work was supported by the Basic Science Research Program through the National Research Foundation of Korea (NRF) funded by the Ministry of Science, ICT & Future Planning (NRF-2015R1C1A1A02037373).

## References

[1] A. Fujishima and K. Honda, "Electrochemical photolysis of water at a semiconductor electrode," *Nature*, vol. 238, no. 5358, pp. 37–38, 1972.

[2] A. J. Bard and M. A. Fox, "Artificial photosynthesis: solar splitting of water to hydrogen and oxygen," *Accounts of Chemical Research*, vol. 28, no. 3, pp. 141–145, 1995.

[3] Y. Park, K. J. McDonald, and K.-S. Choi, "Progress in bismuth vanadate photoanodes for use in solar water oxidation," *Chemical Society Reviews*, vol. 42, no. 6, pp. 2321–2337, 2013.

[4] J. R. Swierk and T. E. Mallouk, "Design and development of photoanodes for water-splitting dye-sensitized photoelectrochemical cells," *Chemical Society Reviews*, vol. 42, no. 6, pp. 2357–2387, 2013.

[5] A. J. Nozik, "Photoelectrochemistry: applications to solar energy conversion," *Annual Review of Physical Chemistry*, vol. 29, pp. 189–222, 1978.

[6] S. K. Pilli, T. G. Deutsch, T. E. Furtak, L. D. Brown, J. A. Turner, and A. M. Herring, "$BiVO_4$/$CuWO_4$ heterojunction photoanodes for efficient solar driven water oxidation," *Physical Chemistry Chemical Physics*, vol. 15, no. 9, pp. 3273–3278, 2013.

[7] D. K. Zhong, S. Choi, and D. R. Gamelin, "Near-complete suppression of surface recombination in solar photoelectrolysis by 'Co-Pi' catalyst-modified W:$BiVO_4$," *Journal of the American Chemical Society*, vol. 133, no. 45, pp. 18370–18377, 2011.

[8] A. Kudo and Y. Miseki, "Heterogeneous photocatalyst materials for water splitting," *Chemical Society Reviews*, vol. 38, no. 1, pp. 253–278, 2009.

[9] A. Kudo, K. Omori, and H. Kato, "A novel aqueous process for preparation of crystal form-controlled and highly crystalline $BiVO_4$ powder from layered vanadates at room temperature and its photocatalytic and photophysical properties," *Journal of the American Chemical Society*, vol. 121, no. 49, pp. 11459–11467, 1999.

[10] J. Su, L. Guo, N. Bao, and C. A. Grimes, "Nanostructured $WO_3$/$BiVO_4$ heterojunction films for efficient photoelectrochemical water splitting," *Nano Letters*, vol. 11, no. 5, pp. 1928–1933, 2011.

[11] A. J. E. Rettie, H. C. Lee, L. G. Marshall et al., "Combined charge carrier transport and photoelectrochemical characterization of BiVO4 single crystals: Intrinsic behavior of a complex metal oxide," *Journal of the American Chemical Society*, vol. 135, no. 30, pp. 11389–11396, 2013.

[12] F. F. Abdi, L. Han, A. H. M. Smets, M. Zeman, B. Dam, and R. V. D. Krol, "Efficient solar water splitting by enhanced charge separation in a bismuth vanadate-silicon tandem photoelectrode," *Nature Communications*, vol. 4, article 3195, 2013.

[13] W. Luo, Z. Yang, Z. Li et al., "Solar hydrogen generation from seawater with a modified $BiVO_4$ photoanode," *Energy and Environmental Science*, vol. 4, no. 10, pp. 4046–4051, 2011.

[14] H. S. Park, K. E. Kweon, H. Ye, E. Paek, G. S. Hwang, and A. J. Bard, "Factors in the metal doping of $BiVO_4$ for improved photoelectrocatalytic activity as studied by scanning electrochemical microscopy and first-principles density-functional calculation," *Journal of Physical Chemistry C*, vol. 115, no. 36, pp. 17870–17879, 2011.

[15] T. W. Kim and K.-S. Choi, "Nanoporous $BiVO_4$ photoanodes with dual-layer oxygen evolution catalysts for solar water splitting," *Science*, vol. 343, no. 6174, pp. 990–994, 2014.

[16] D. R. Gamelin, "Water splitting: catalyst or spectator?" *Nature Chemistry*, vol. 4, no. 12, pp. 965–967, 2012.

[17] F. L. Formal, K. Sivula, and M. Grätzel, "The transient photocurrent and photovoltage behavior of a hematite photoanode under working conditions and the influence of surface treatments," *The Journal of Physical Chemistry C*, vol. 116, no. 51, pp. 26707–26720, 2012.

[18] K. Sivula, "Metal oxide photoelectrodes for solar fuel production, surface traps, and catalysis," *Journal of Physical Chemistry Letters*, vol. 4, no. 10, pp. 1624–1633, 2013.

[19] F. E. Osterloh, "Inorganic nanostructures for photoelectrochemical and photocatalytic water splitting," *Chemical Society Reviews*, vol. 42, no. 6, pp. 2294–2320, 2013.

[20] C. Liu, N. P. Dasgupta, and P. Yang, "Semiconductor nanowires for artificial photosynthesis," *Chemistry of Materials*, vol. 26, no. 1, pp. 415–422, 2014.

[21] H. Ye, H. S. Park, and A. J. Bard, "Screening of electrocatalysts for photoelectrochemical water oxidation on W-doped $BiVO_4$ photocatalysts by scanning electrochemical microscopy," *Journal of Physical Chemistry C*, vol. 115, no. 25, pp. 12464–12470, 2011.

[22] G. Qui, Z. Gao, H. Yin, X. Feng, W. Tan, and F. Liu, "Synthesis of $MnPO_4.H_2O$ by refluxing process at atmospheric pressure," *Solid State Sciences*, vol. 12, no. 5, pp. 808–813, 2010.

[23] K. J. McDonald and K.-S. Choi, "A new electrochemical synthesis route for a BiOI electrode and its conversion to a highly efficient porous $BiVO_4$ photoanode for solar water oxidation," *Energy and Environmental Science*, vol. 5, no. 9, pp. 8553–8557, 2012.

[24] J. Baltrusaitis, D. M. Cwiertny, and V. H. Grassian, "Adsorption of sulfur dioxide on hematite and goethite particle surfaces," *Physical Chemistry Chemical Physics*, vol. 9, no. 41, pp. 5542–5554, 2007.

[25] T. Yamashita and P. Hayes, "Analysis of XPS spectra of $Fe^{2+}$ and $Fe^{3+}$ ions in oxide materials," *Applied Surface Science*, vol. 254, no. 8, pp. 2441–2449, 2008.